SUPPLEMENTARY MATERIAL

Understanding luminescence properties of grain boundaries in GaN thin films and their atomistic origin

Fig. S1 shows total electronic density of states (DOS) of GaN that has bulk-like structure which we present here to compare with those of the GaN having defect structures such as dislocations or grain boundaries. After structural relaxation, the equilibrium lattice parameters of a=3.186 Å and c=5.187 Å were obtained, in which the consistency with the reference values verifies the reliability of our calculation results. According to the DOS obtained here, the band gap of bulk GaN was lower than reference value of 3.4 eV, and this band gap underestimation is universally observed tendency in previous DFT calculations. Since we were only interested in examining electronic structure variation in qualitative manner, we did not add additional energy terms to modify the band gap energy to be exactly equivalent to reference value. Here, localized states were not observed in the DOS as shown in Fig. S1, exhibiting different behavior in comparison with those of defect structures such as grain boundaries and threading dislocations.

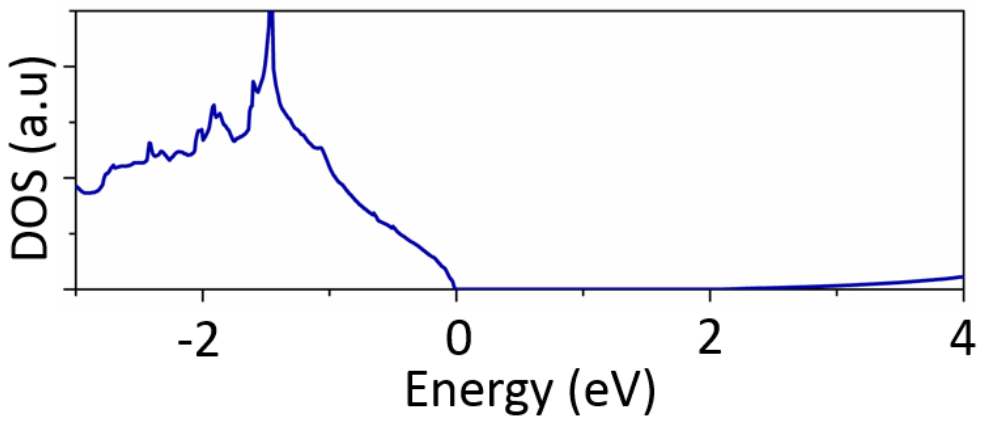

FIG. S1. Density of states obtained for single crystalline GaN.

Structural models for threading dislocations were constructed to investigate the formation energy and electronic DOS. Figs. S2(a) and (b) show atomic structure of the edge dislocation having open-core structure and its corresponding total DOS. The DOS exhibits additional localized states near the valence band and above the conduction band in comparison with those of bulk-like structure. In contrast, DOS obtained for the edge dislocation having full-core structure (Figs. S2(c) and (d)) showed no distinguished localized states within the band gap which is in consistent with the previous calculation studies.[1]

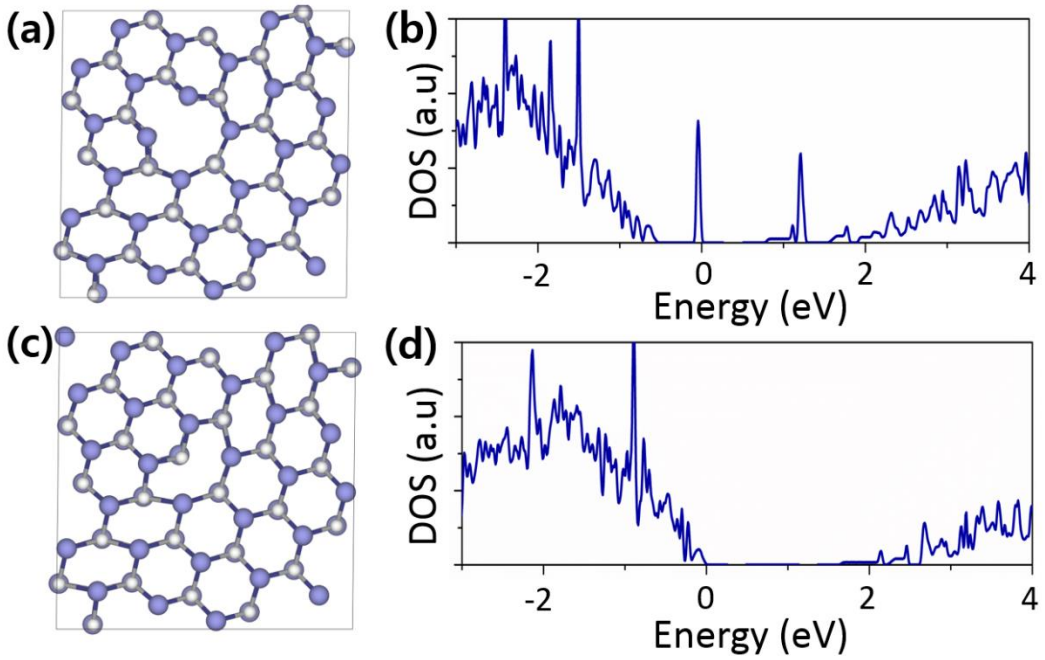

FIG. S2. Density of states obtained for edge dislocation in GaN. (a) Structural model for open core structure configuration of the edge dislocation and (b) its corresponding density of states. (c) Structural model for full core structure configuration of the edge dislocation and (d) its corresponding density of states.

Energetically stable positions for the formation of point defects in the high-angle grain boundary were investigated by total energy calculation. Figs. S3(a) and (b) show atomic configurations of the unit cells containing Σ=7 boundaries composed of open-core structure and full-core structure, respectively. Compared with the unit cells shown in Figs. 3(a) and (b), the size of the unit cells shown in Figs. S3(a) and (b) was expanded to keep the vacancy farther away from other vacancies, and thereby minimize the interaction between them. The dimensions of the unit cell was doubled along the two directions; it was doubled along the directions parallel to the grain boundary direction (core to core direction) and along the out-of-plane direction. Here, the formation energies of single Ga vacancy and N vacancy was calculated at every possible atomic column position designated with the numbers as shown in Figs. S3(a) and (b). The formation energies of those vacancies calculated for open-core boundary and full-core boundary were plotted in Figs. S3(c) and (d), respectively. As shown in Fig. S3(c), the most favorable position to form Ga and N vacancy in open-core boundary is on the atomic column indicated with the number 4 shown in Fig. S3(a). In the case of full-core boundary, the most favorable position to form Ga and N vacancy is on the atomic column marked with the number 2 presented in Fig. S3(b). According to the calculation results, it was shown that the point defects such as Ga and N vacancy prefer to form in core region of the high-angle grain boundaries.

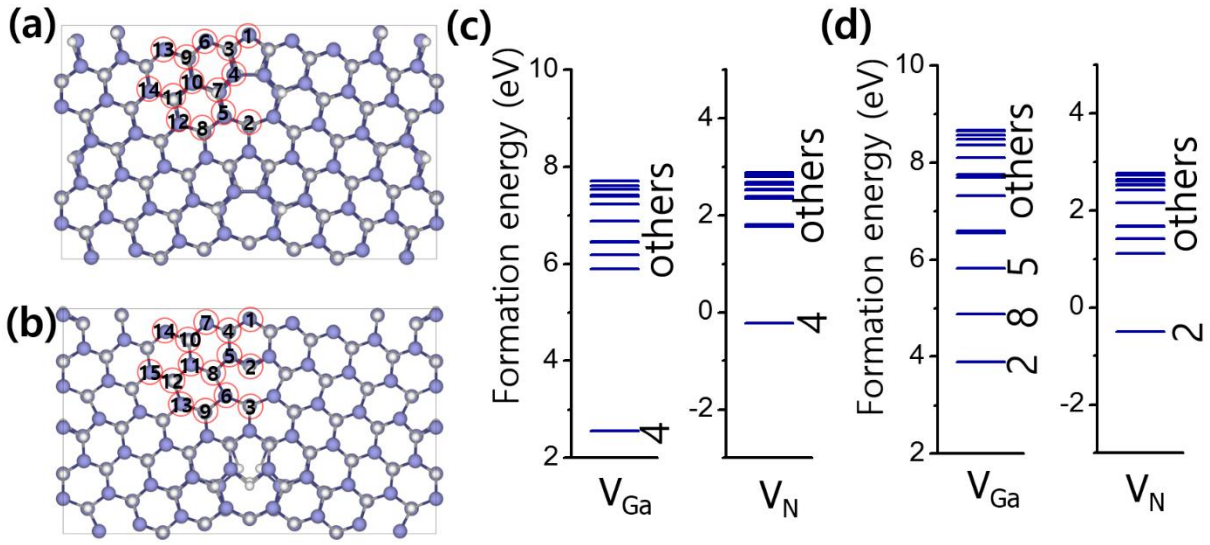

FIG. S3. Structural models for Σ=7 boundary composed of (a) open-core structures and (b) full-core structures with each position of the atomic columns indicated with red circles and the numbers. Formation energies of single Ga and N vacancies at the atomic column positions indicated with the red circles and the numbers in (c) open-core boundary shown in Fig. S3(a) and (d) full-core boundary shown in Fig. S3(b).

We also performed additional calculations for the case with the higher concentration of vacancies to figure out how the multiple vacancies are arranged in the grain boundaries. Here, the Ga or N vacancy was already formed in the energetically favorable position that we just investigated as marked with the blue circles in Figs. S4(a) and (b). Given this configuration, the formation energies of second Ga and N vacancies were calculated for the open-core and full-core boundaries as shown in Figs. S4(c) and (d), respectively. In the case of open-core boundary, both Ga and N vacancy prefer to be formed in atomic column indicated with the number 4, and in the case of full-core boundary, they prefer to be formed in the atomic column indicated with the number 2. We believe that this calculation results indicate a tendency of vacancy accumulation on the core region of the grain boundaries.

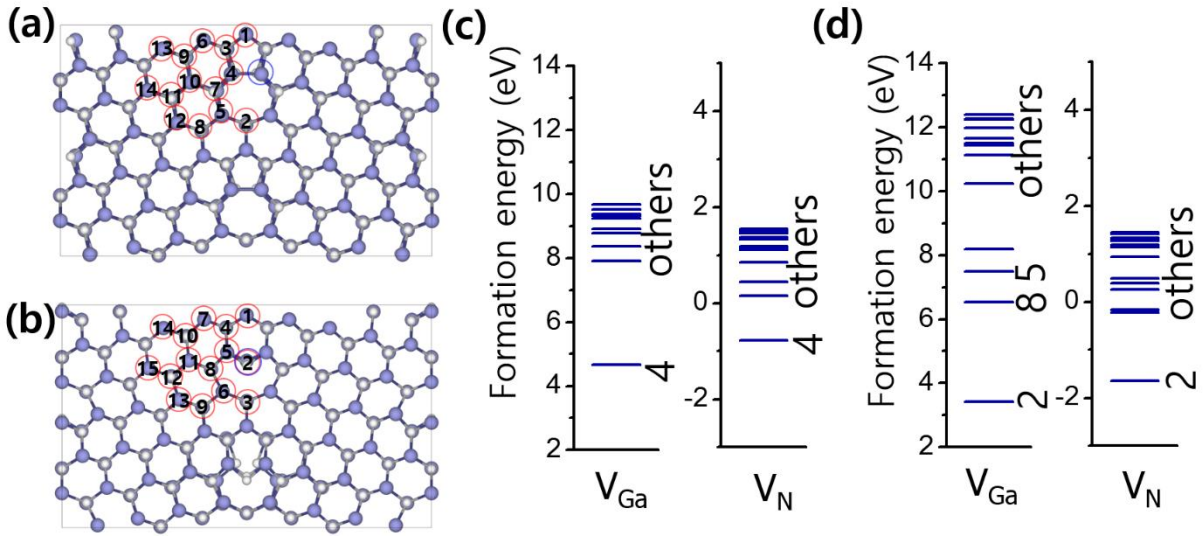

FIG. S4. Structural models for Σ=7 boundary composed of (a) open-core structures and (b) full-core structures with each position of the atomic columns indicated with red circles and the numbers. Single Ga or N vacancy was already formed in atomic column indicated with blue circle. Formation energies of additional Ga and N vacancies at the atomic column positions indicated with the red circles and the numbers in (c) open-core boundary and (d) full-core boundary.

Electronic structure variations accompanied with the formation of point defects in the grain boundaries were further investigated. We examined total electronic DOS for the Σ=7 boundaries composed of open-core and full-core structures (Figs. S5a and b) after forming single Ga or N vacancy in the atomic column marked with red circle, and subsequently forming second Ga or N vacancy in the atomic column marked with blue circle (Figs. S5c–j). In Figs. S5c–j, we also presented core structures obtained after structural relaxation with the formation of each vacancy. Those sites on which the first and second Ga/N vacancies are to be formed were verified as energetically most favorable site according to the total energy calculations as we discussed above. Here, we focused on the DOS variation within the band gap including mid-gap states which are strongly associated with the luminescence properties. In the case of the open-core boundary shown in Fig. S5(a), additional mid-gap states were formed after forming first Ga vacancy as indicated with arrows in Fig. S5(c) although they were not observed after forming second Ga vacancy as shown in Fig. S5(d). When a N vacancy was formed in the open-core boundary, additional mid-gap state was formed just above valence band as indicated with arrow in Fig. S5e. Moreover, another mid-gap state was also observed near the conduction band after forming second N vacancy at the core even though the mid-gap state formed when the first N vacancy was formed were not observed in this case. In the case of full-core boundary, although no mid-gap states were formed after forming first Ga vacancy at the core, two mid-gap states were observed after forming second Ga vacancy as shown in Figs. S5(g) and (h). When we form a N vacancy in the full-core boundary, we observed an additional mid-gap state marked with arrow in Fig. S5(i), and it shows similar shape after forming second N vacancy as shown in Fig. S5(j). In short, the electronic structures of the grain boundaries change with a general tendency of the additional mid-gap state formation within the band gap and their variation. Those mid-gap state variation along with the formation of

point defects would play a significant role in understanding luminescence properties of the grain boundaries in GaN films.

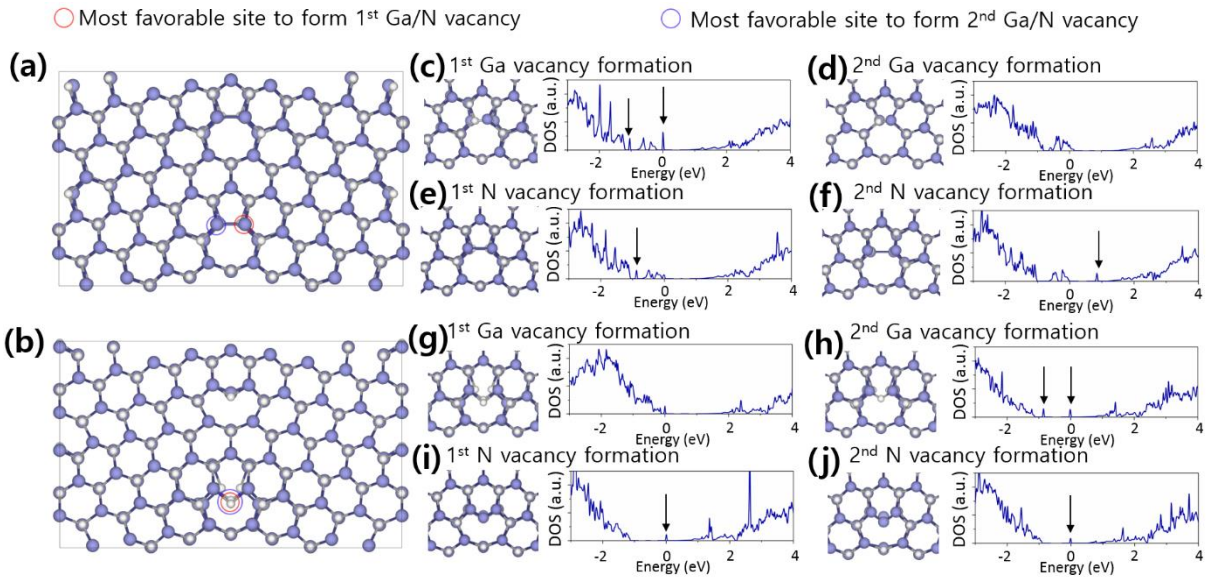

FIG. S5. Structural model for Σ=7 boundaries composed of (a) open-core structures and (b) full-core structures. The atomic column indicated with red circle is the most favorable site to form 1st Ga or N vacancy and the atomic column indicated with blue circle is the most favorable site to form 2nd Ga or N vacancy given the 1st vacancy formed in red circled region. (c) Relaxed structure after forming 1st Ga vacancy at the core region of the open-core boundary and its corresponding density of states (DOS). (d) Relaxed structure after forming 2nd Ga vacancy at the core region and its corresponding DOS. (e) Relaxed structure after forming 1st N vacancy at the core region of the open-core boundary and its corresponding DOS. (f) Relaxed structure after forming 2nd N vacancy at the core region and its corresponding DOS. (g) Relaxed structure after forming 1st Ga vacancy at the core region of the full-core boundary and its corresponding DOS. (h) Relaxed structure after forming 2nd Ga vacancy at the core region and its corresponding DOS. (i) Relaxed structure after forming 1st N vacancy at the core region of the full-core boundary and its corresponding DOS. (j) Relaxed structure after forming 2nd N vacancy at the core region and its corresponding DOS.

Figs. S6 (a) and (b) are unfiltered and band-pass filtered high-angle annular dark field (HAADF) scanning transmission electron microscopy (STEM) images. Band pass filtering was used to remove high- and low-frequency features in images to get rid of noise and visualize the core structures more clearly. As a result, we can clearly identify the atomic positions of the grain boundary core structures. Then, we estimated the intensities of each atomic column constituting the grain boundaries to compare with the theoretical calculation results. Since the quantitative information might be lost or biased in band-pass filtered images, we used unfiltered raw data to estimate the intensity. 6 different positions of atomic columns constituting open-core structure were indicated with the numbers in the inset of Fig. S6 (b). Total intensities for each atomic column were measured from the unfiltered HAADF STEM image (Fig. S6 (a)) and plotted in Fig. S6 (c). Atomic column #3 exhibited lowest total intensity which is consistent with the most favorable sites to form vacancies in open-core structures predicted by our theoretical calculation.

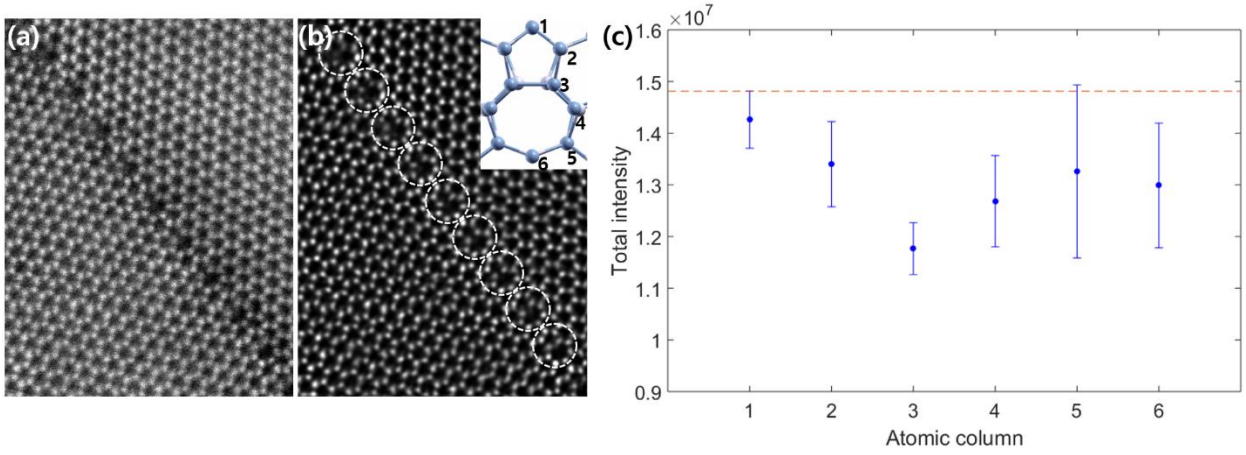

FIG. S6. High-angle annular dark field (HAADF) scanning transmission electron microscopy (STEM) analysis on Σ=7 boundaries. (a) Unfiltered and (b) band-pass filtered HAADF STEM images of Σ=7 boundaries. The inset in (b) shows schematic diagram of open-core structures with individual atomic columns marked with numbers. (c) Total intensities of the individual atomic columns estimated from 9 different open cores marked with dashed circles in (b). Total intensities

were obtained from raw data shown in (a). Red dashed line indicates the total intensity value obtained from the atomic columns in bulk region.

Unfiltered and band-pass filtered HAADF STEM images shown in Figs. S7 (a) and (b) are the same sets of data shown in Fig. 2 (d). To estimate the intensity of each atomic column, we used unfiltered raw HAADF STEM image shown in Fig. S7 (a) and plotted in Fig. S7 (c). Atomic column #7 showed lowest intensity, which was consistent with the most favorable sites to form vacancies in full-core structures predicted by our theoretical calculation.

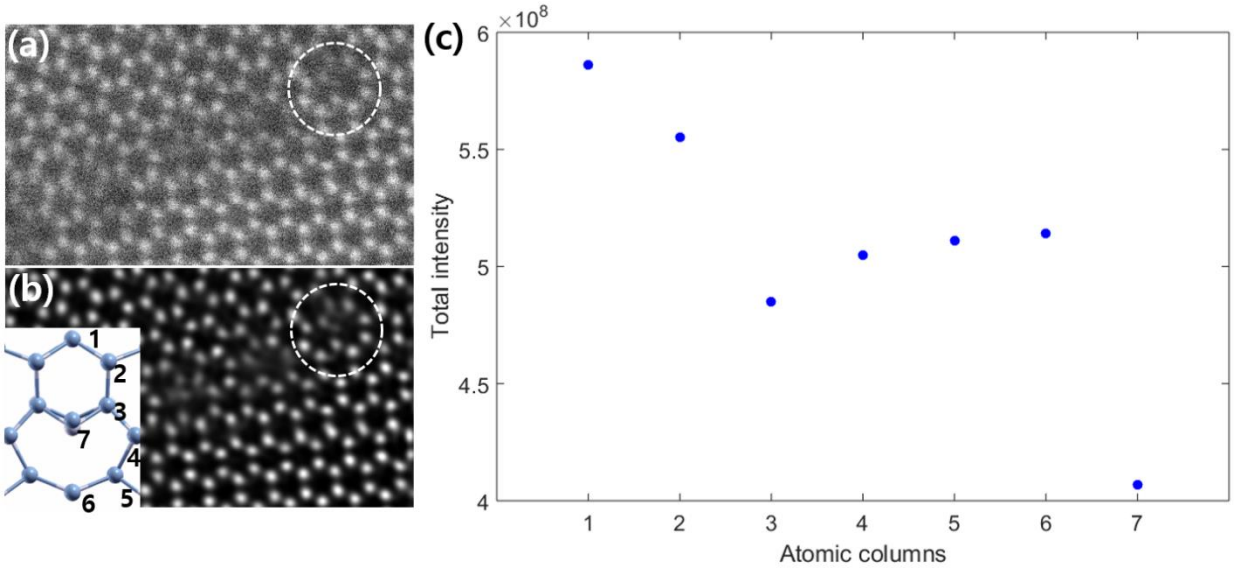

FIG. S7. High-angle annular dark field (HAADF) scanning transmission electron microscopy (STEM) analysis on Σ=7 boundaries. (a) Unfiltered and (b) band-pass filtered HAADF STEM images of Σ=7 boundaries. The inset in (b) shows schematic diagram of full-core structures with individual atomic columns marked with numbers. (c) Total intensities of the individual atomic columns estimated from the single core marked with dashed circles in (a) and (b). Total intensities were obtained from raw data shown in (a).

[1] J. Elsner, R. Jones, P. Sitch, V. Porezag, M. Elstner, T. Frauenheim, M. Heggie, S. Ö berg, and P. Briddon, Phys. Rev. Lett. 79, 3672 (1997).